Chemico-Viscous Remanent Magnetization in the Fe_3O_4-γFe_2O_3 System

ÖZDEN ÖZDEMIR AND DAVID J. DUNLOP

The chemical remanent magnetization (CRM) acquired when single-domain size magnetite (Fe_3O_4) oxidizes to maghemite (γFe_2O_3) in a 50-microtesla field at a series of 13 temperatures from 100° to 656°C is of similar intensity to viscous remanent magnetization (VRM) acquired under the same field and temperature conditions by unoxidized magnetite. The remanences of the oxidized and unoxidized phases also have similar resistances to demagnetization. These similarities imply that the remanence of the oxidized material is a chemico-viscous remanent magnetization (CVRM) having some of the characteristics of both classic growth CRM and thermally activated VRM. At low temperatures in partially oxidized grains, VRM of the magnetite core and growth CRM of the maghemite surface layer contribute about equally to CVRM. Near the Curie point, intensity of CVRM increases to a Hopkinson-type peak. High-temperature CVRM is more resistant to demagnetization than the thermoremanent magnetization (TRM) produced from cooling through the Curie point.

CRYSTALLIZATION OR CHEMICAL remanent magnetization (CRM) produced when a ferromagnetic mineral grows to stable single-domain (SD) size in the presence of a magnetic field commonly overprints part of the primary remanence of rocks. The recognition and removal of CRMs are vital to the success of paleomagnetic studies of ancient orogens and their foreland zones. CRMs acquired during the transformation of a magnetic parent mineral within ~100°C of the Curie temperature seem to have an acquisition mechanism similar to that of viscous remanent magnetization (VRM) (*1, 2*), which is produced by prolonged exposure to a field without grain size change. At ordinary temperatures, VRM is acquired by a small fraction of SD grains just above the superparamagnetic (SP) threshold diameter d_s for thermal stability, whereas CRM, in the simplest case (*3*), is blocked in practically all grains as they grow beyond d_s to possibly quite large terminal sizes. In this situation, CRM should be more intense and more resistant to demagnetization than VRM. With heating, the thermal stability of a particle decreases, until at the unblocking temperature T_{UB}, the particle becomes SP and its remanence disappears (*4*). Equivalently, d_s increases with rising temperature until at T_{UB} it has swept through the sample size spectrum and destabilized all particle remanences. At temperatures just below T_{UB}, a large fraction of the grains have d just above d_s and readily acquire VRM. If a new phase grows at this temperature, its terminal size will likewise be just above d_s. The CRM it acquires by growing through d_s will be continuously augmented by VRM. The size-controlled (CRM) and time-controlled (VRM) processes merge.

We propose the term chemico-viscous remanent magnetization (CVRM) to describe this remanence process. There is a practical reason for this new term. It is generally assumed in paleomagnetism that chemical remagnetization of rocks and viscous or thermoviscous remagnetization are distinct processes. For purely thermoviscous remagnetization, peak demagnetizing temperatures can be used to reconstruct regional thermal histories (*5*) and estimate depths of burial (*6*). In many settings, however, some chemical alteration has clearly taken place. If the relation between high-temperature VRM and CVRM can be quantified, it may be possible to recalibrate the method for use with CRM-CVRM overprints.

In this report, we compare the properties of CRM-CVRM produced from the oxidation of SD-size magnetite (Fe_3O_4) to maghemite (γFe_2O_3) at low and high temperatures with those of pure VRM in unoxidized parent magnetite. The oxidation of magnetite in rocks is probably the most common mineral alteration with which paleomagnetists have to contend. This reaction also proceeds at a reasonable rate at only moderately elevated temperatures if the particle size is small.

Our starting material consisted of single-crystal cubes of magnetite grown in aqueous solution (*7–9*). We measured VRMs on 2% by weight dispersions of oxide in a CaF_2 matrix. Samples were hydraulically pressed into small cylindrical pellets and sealed in evacuated capsules to prevent oxidation during heating. A second set of pellets, prepared and pressed in the same way but unsealed and heated in air, was used in CRM-CVRM experiments. Before beginning experiments, we demagnetized the

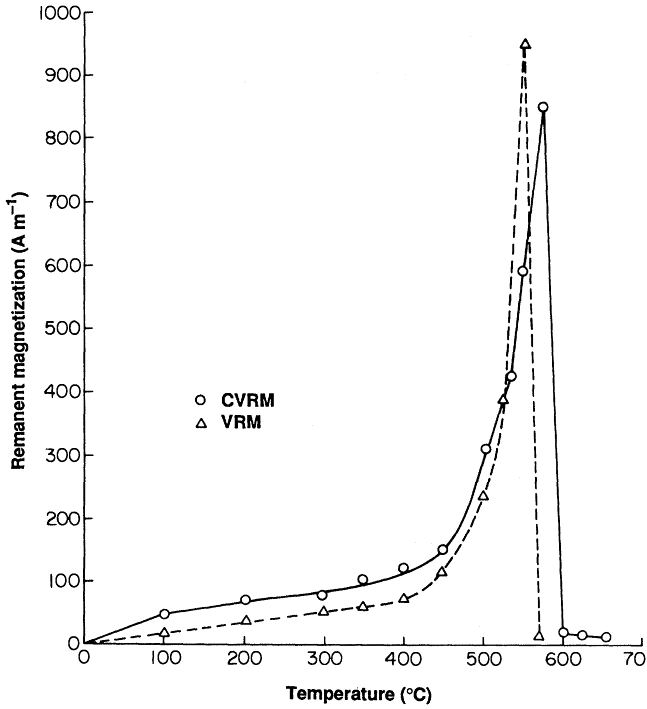

Fig. 1. A comparison of the intensities of CVRM of oxidized or partially oxidized magnetite with those of VRM of unoxidized magnetite after 2.5-hour heatings at the same temperature *T*.

Geophysics Laboratory, Department of Physics, University of Toronto, Toronto, Canada M5S 1A7.

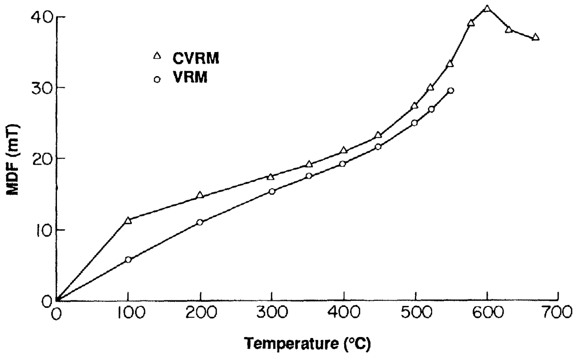

Fig. 2. A comparison of median destructive fields of CVRM and VRM after runs at the same temperature.

samples in a peak alternating field (AF) of 100 mT. In each run, we produced VRM and CRM-CVRM under identical time and temperature conditions by heating fresh companion sealed and unsealed samples in null field to a given temperature *T*, maintaining the temperature constant for 2.5 hours while applying a field *H* of 50 μT along the axis of either pellet, and finally cooling in null field to room temperature (*10*). There were 13 runs at temperatures ranging from 100° to 656°C, as well as a VRM run at 20°C.

The intensity of VRM (M_{VRM}) increased quasi-exponentially as *T* increased, peaked at a value of 950 A m^{-1} (per unit volume of magnetite) after the 552°C run, then decreased abruptly (Fig. 1). The intensity of CVRM (M_{CVRM}) changed in a similar way. It reached a peak value of 860 A m^{-1} after the 576°C run, then dropped sharply to 26 A m^{-1} after the 605°C run.

Demagnetization by AF in steps to 100 mT showed that all VRMs and CVRMs were univectorial remanences parallel to *H*. The median destructive field (MDF) of VRM increased from 7.5 to 29.5 mT as the temperature of the run increased from 100° to 552°C (Fig. 2). The MDF of CVRM increased in a similar way, from 11.5 mT after the 100°C run to 41 mT after the 605°C run. With further heating, the MDF of CVRM decreased.

For comparison, we demagnetized an AF-thermoremanent magnetization (TRM) produced by cooling a fresh vacuum-sealed sample in a 50-μT field from above the magnetite Curie temperature. The resistance of this TRM was similar to that of the VRM produced at 552°C, but was considerably softer than the resistance of the CVRM produced at the same temperature (Fig. 3).

Hysteresis, x-ray, and thermomagnetic analyses, indicate that the sealed VRM samples did not change appreciably as a result of heating. For the unsealed samples, three different phase assemblages were observed (Fig. 4 and Table 1). In heatings between 20° and 300°C, magnetite partially oxidized to maghemite. The M_S values decreased from 92 to 75 A m^2 kg^{-1}, the reference value for maghemite (*11*), and the lattice parameter decreased to ~8.34 Å (maghemite), although the Curie temperature T_c increased only slightly, to ~582°C. Double (440) reflections after the 200° and 300°C runs with *d* spacings of 1.475 and 1.485 Å indicate that distinct spinel phases had formed, probably a core of essentially unoxidized magnetite inside a surface shell of maghemite (*12, 13*). Oxidation in the 300° to 453°C range resulted in total conversion to the single phase maghemite. Both M_S values and x-ray parameters remained constant over this range. Above 453°C, maghemite began to invert to weakly magnetic hematite (Table 1). The M_S values indicate about 40% hematite and 60% maghemite after the 656°C run. Curie temperatures of the spinel phase were 602° to 614°C after these runs, compared to 590°C (*14, 15*) to 645°C (*16*) for maghemite.

An unanticipated result was that the intensities and AF stabilities of CRM-CVRM were similar to those of VRM in all runs, not just the high-temperature ones (Figs. 1 and 2). For this reason, we extend the term CVRM to include low-temperature as well as high-temperature remanences. In the range of partial oxidation (after heatings to 100° to 300°C), the measured CVRM of our magnetite-maghemite mixture was only a factor of 2 greater than the VRM produced in single-phase magnetite at the same temperature (Fig. 1). The difference $\Delta M = M_{\mathrm{CVRM}} - M_{\mathrm{VRM}}$ presumably represents pure CRM acquired in a nonviscous fashion. After the 100°C run, CVRM was about twice as resistant as VRM to AF cleaning (Fig. 2), but the difference in hardness diminished in higher temperature runs.

In low-temperature runs, VRM and growth CRM processes may proceed independently in the same grain. The growing surface shell of maghemite will experience not only the externally applied field but also the strong back field of the SD magnetite core (*17*). Our samples were initially demagnetized, thus individual magnetite SD moments were oriented at random. Core-shell interactions ensured that the directions of CRMs acquired by the growing maghemite shells were also largely randomized, apart from the biasing effect of the external field. As maghemite grows, magnetite cores shrink in size and in some grains may become quite viscous. Thus in the 20° to 300°C (two-phase) range, separate magnetite VRM and maghemite CRM contributions to the CVRM are likely.

The MDFs of CVRM and VRM are different in low-temperature runs because the room-temperature SP-SD critical size d_s for maghemite is around 250 Å, but particles had diameters up to 650 Å. Grains that acquired CRM at low temperatures may have grown considerably beyond critical size and were thus more coercive than the nearly SP grains carrying VRM, whose coercivities were reduced by thermal activation (*18*). The contrast in coercivity decreased in higher temperature runs because d_s increases with rising temperature, so that the sizes of maghemite grains or regions of grains carrying CRM began to approach the critical blocking volume. Their coercivities were

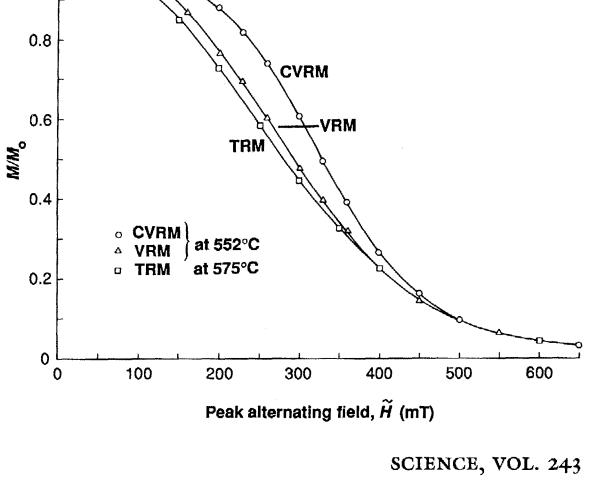

Fig. 3. Comparative AF demagnetization curves for VRM and CVRM produced in sealed and unsealed samples, respectively, in runs at 552°C and for total TRM produced in a sealed sample cooled from above 575°C to room temperature. A field of 50 μT was applied in all cases.

Table 1. Curie temperature T_c, lattice parameter a determined from spinel X-ray reflections, and other magnetic phases present, with the X-ray lines by which they were identified, for the starting material and after oxidation in runs at various temperatures T; (*hkl*) are crystal plane indices.

T (°C)	T_c (°C)	Spinel a (Å)	Other phases (*hkl*)
20	575	8.393 ± 0.008	
200	582	8.336 ± 0.007	Fe_3O_4 (440)
300	581	8.339 ± 0.007	Fe_3O_4 (440)
453	602	8.337 ± 0.010	
576	614	8.333 ± 0.010	αFe_2O_3 (104)
605	610	8.334 ± 0.010	αFe_2O_3 (104), (110)

accordingly reduced by the thermal fluctuation field (*18*). At 300°C, CVRM and VRM have similar MDFs.

In the oxidation of some magnetites and titanomagnetites (*1, 19*), CRMs remained parallel to an initial remanence even when quite strong fields were applied in other directions, as a result of exchange coupling between parent and daughter phases. In our experiments, we purposely randomized any phase-coupled remanence inherited from the parent magnetite by demagnetizing the samples initially, but the magnetite core and maghemite shell could act as a coupled unit in acquiring a new remanence. If such coupling occurs, because magnetite and maghemite have similar critical blocking sizes d_s, there is little scope for the acquisition of growth CRM unless the grains themselves grow during oxidation.

Some crystal growth does accompany maghemitization. During oxidation, one-ninth of the Fe diffuses to the surface to form new unit cells of maghemite, and the crystal volume increases by about 11% (*20*). The small difference in d_s values between magnetite and maghemite (or between titanomagnetite and titanomaghemite) has been theorized to cause some originally SD grains to become SP upon maghemitization (*21*). However, the volume increase upon oxidation more than compensates for the change in d_s. Marked increases in M_{RS}/M_S values [see also (*22*)] and corresponding decreases in H_{CR}/H_C values after the 100° and 200°C runs (Fig. 4B) indicate that the proportion of SD grains had increased. Bulk coercive force H_C also increased from 100° to 200°C [Fig. 4C; see also (*15, 23*)]. These changes cannot result from subdivision of originally MD grains, because the MD fraction is small; therefore, SP grains must be growing to stable SD size.

If partially oxidized grains behave magnetically as a unit, a fraction of them could acquire CRM in growing from SP to SD size. They could not grow much beyond d_s, however, and the MDF of CVRM should be similar to the MDF of VRM in the original magnetite.

Knowles (*13*) has shown that the volume change during maghemitization causes stress between the magnetite core and maghemite surface layer and that this stress is sufficient to account for the increase in H_C in partially oxidized grains (for example, Fig. 4C). It may also account for some of the twofold contrast between the MDFs of magnetite VRM and maghemite-magnetite CVRM observed after the 200°C run. At higher temperatures, where oxidation approaches completion, the stress will diminish and with it the contrast in MDFs.

From 300° to 453°C, changes in the MDFs of CVRM and VRM closely match changes in bulk coercivity H_C. Small but appreciable differences in the degree of oxidation and grain growth apparently occur over this range.

From 453° to 605°C, the intensities and coercivities of VRM and CVRM are almost identical, apart from a temperature shift attributed to the difference between the magnetite and maghemite Curie points (575° and 610°C, respectively). Both remanences exhibit Hopkinson-type peaks (*24*) just below the Curie point because the particles, which are magnetically blocked at ordinary temperatures, have been heated close to their unblocking temperatures T_{UB} (*4*). They are then easily activated by small fields on a laboratory time scale (*4*).

Similarly VRMs produced at high temperatures are more resistant to AF demagnetization at room temperature (Fig. 2) because their high-temperature magnetic states have been blocked or stabilized by cooling in zero field to room temperature [see (*25*) for analogous results for partial TRMs]. Our study also demonstrates that high-temperature VRM and CVRM have AF stabilities that equal or exceed those of TRM, which has usually been considered the most stable remanence of igneous rocks.

The peak in CVRM intensity of maghemite matches closely the peak in VRM intensity of magnetite (Fig. 1). The peak CVRM intensity is slightly lower, probably because M_S is lower for maghemite than for magnetite. The CVRM peak is also shifted to higher temperatures by about 25°C, which is about the same as the difference in Curie points of the two minerals. The enormous increase of CVRM intensity in high-temperature runs compared to low-temperature runs cannot be related to the appearance of hematite among the reaction products because hematite is too weakly magnetic. Nor can it be accounted for by the kinetics of the $Fe_3O_4 \rightarrow \gamma Fe_2O_3$ reaction, because the time available during the reaction for thermally activated magnetization changes is considerably shorter at the higher temperatures. The deciding factor, as with simple VRM, must be that in the unblocking temperature range, d_s is close to the

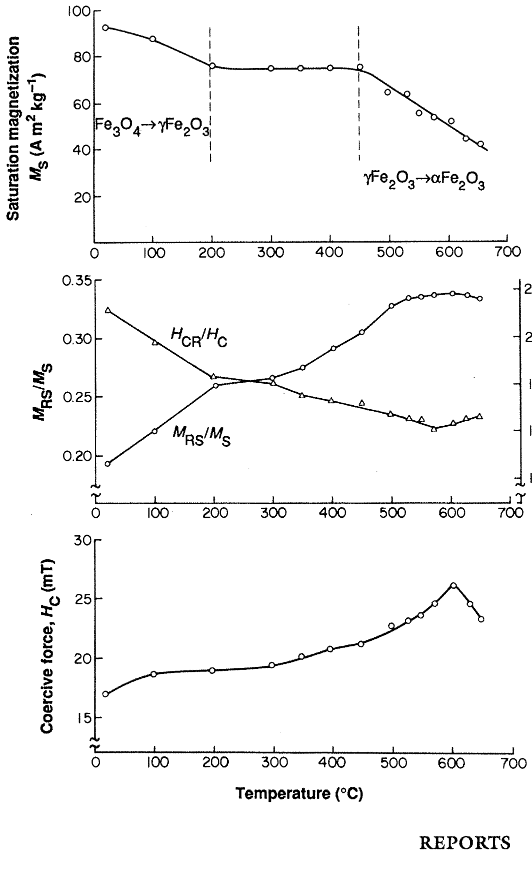

Fig. 4. Room-temperature hysteresis properties of unsealed samples, measured initially and after CVRM runs at 13 different temperatures; (**A**) saturation magnetization M_S; (**B**) saturation remanence ratio M_{RS}/M_S and coercivity ratio H_{CR}/H_C; (**C**) bulk coercive force H_C.

particle size *d*. Despite the rapidity with which the daughter phase grows to terminal size, it no longer grows past a sharply defined critical size that blocks all further magnetization changes. Instead, the remanence continues to evolve viscously. We conclude that high-temperature CVRM owes most of its intensity to VRM of particles of the daughter phase, acquired after they have grown to terminal size.

At low temperatures, where oxidation is incomplete, CVRM probably consists of coexisting CRM in one phase and VRM in the other. At high temperatures, where no parent magnetite survives, the blocking mechanism of CVRM changes from the sharp, critical-volume process associated with conventional CRM to a gradual, continuous process. At these temperatures, the efficiency increases enormously: the CVRM after the 576°C run was about ten times as intense as the CVRM produced at 200° and 300°C with the same experimental setup. The MDF of the 576°C CVRM is more than twice the MDF of the CVRM at 200° to 300°C. The bulk coercivity H_C increased by about 30% from 300° to 576°C and can account for only a small part of the increase in MDF. Most of the increase is a strictly viscous enhancement resulting from longer exposure time to the field (*26*). As for VRM, high-temperature CVRM is harder and more intense than low-temperature CVRM.

The inversion of maghemite to hematite had only a minor effect on CVRM in our experiments. In the run at 576°C, the temperature of the CVRM peak, only about 25% of the sample inverted to hematite (Fig. 4A). If inversion were a gradual process affecting large and small grains equally, the decrease in residual maghemite volumes should have shifted the entire T_{UB} spectrum to lower temperatures compared to the magnetite spectrum. No such shift was seen in our experiments. Inversion in its initial stages probably converts small grains completely to hematite while leaving large grains almost unaffected.

For high degrees of inversion, several workers (*27*) have measured anomalously high CRMs that they attributed to exchange coupling between maghemite and hematite, although they suggested no mechanism by which these lattices, with their incompatible structures, cell dimensions, and directions of easy magnetization, could couple. In previous experiments on this system (*1, 2*), we found no compelling evidence for phase coupling, but we could not rule it out either. The results of the CVRM runs from 605° to 656°C provide new evidence. A coupled maghemite-hematite particle should be thermally stable in at least part of this range, because its T_{UB} should be intermediate between the T_{UB}'s of either mineral separately. Unblocking temperatures for SD hematite are generally within 30°C of the hematite Curie temperature of 675°C, and T_{UB} for a coupled particle should rise as the hematite fraction increases. Experimentally, however, CVRM intensity decreased from 860 A m^{-1} after the 576°C run to only 25.5 A m^{-1} after the 605°C run, and decreased still further in subsequent runs. The maghemite alone, and not the two phases acting in combination must control the acquisition of CVRM. Furthermore, the MDF of CRM, measured at room temperature, decreased continuously between the 605° and 656°C runs. If the magnetically softer maghemite were exchange coupled to high-coercivity hematite, the MDF should increase with increasing hematite fraction. The change in MDF and the parallel changes in H_C and the H_{CR}/H_C and M_{RS}/M_S ratios can be accounted for, however, if the phases act independently. As hematite regions grow, maghemite regions shrink and pass from SD to SP.

It has been thought that anomalously intense and stable CRM produced experimentally in the γFe_2O_3-αFe_2O_3 system around 550°C was the outcome of exchange coupling between the phases. We find, however, that high remanence values and AF stabilities result whenever maghemite is produced well above ambient temperatures. Inversion of our material to αFeO_3 was much less than in earlier experiments (*1, 2, 27*), and the presence of a second phase was shown to be irrelevant. Much of the maghemite CRM is acquired by a VRM mechanism, and time rather than volume change is the key factor in its acquisition. The striking Hopkinson-type peak in maghemite CRM intensity at high temperatures is therefore a manifestation of thermal activation close to the unblocking temperature (*4*). Chemico-viscous remanence seems to be an appropriate term to describe this phenomenon. When these CVRMs or VRMs are cooled to room temperature, the high-temperature state is blocked and the remanence becomes resistant to AF demagnetization, its stability exceeding even the stability of TRM.

If produced at or just above room temperature, CVRMs do not have as great an enhancement of intensity and stability but are still considerably stronger and more coercive than room-temperature VRMs. Low-temperature CVRM seems to comprise two components: conventional CRM acquired by the growing maghemite and VRM of the residual magnetite. Stress associated with expansion of the maghemite lattice imparts higher coercivities to partially oxidized crystals than to monophase ones. For this reason, coercivities of CVRM in Fe_3O_4-γFe_2O_3 grains are significantly higher than those of VRM in either phase separately at the same temperature.

In nature, both VRM and CVRM may be much enhanced by high temperatures at lower crustal depths. The Hopkinson peak in VRM has been considered recently by workers attempting to explain large, long-wave length magnetic field anomalies detected by the MAGSAT satellite (*28*), but the analogous CVRM enhancement needs to be investigated. The VRMs and CVRMs acquired by rocks buried tectonically at more modest depths and later exhumed can be resistant to AF cleaning. High-temperature CVRM overprints may actually be harder than the TRM they replace. Orogenic burial and uplift remagnetization are now recognized as severe contaminants of the paleomagnetic record (*29*). Additional experiments are needed to compare and calibrate thermoviscous and chemico-viscous overprinting in rocks.

REFERENCES AND NOTES

1. Ö. Özdemir and D. J. Dunlop, *J. Geophys. Res.* **90**, 11513 (1985).
2. ———, *ibid.* **93**, 6530 (1988).
3. K. Kobayashi, *J. Geomagn. Geoelectr.* **12**, 148 (1961).
4. L. Néel, *Ann. Geophys.* **5**, 99 (1949).
5. G. W. Berger, D. York, D. J. Dunlop, *Nature* **277**, 46 (1979); E. McClelland-Brown, *Geology* **9**, 112 (1981).
6. G. Pullaiah, E. Irving, K. L. Buchan, D. J. Dunlop, *Earth Planet. Sci. Lett.* **28**, 133 (1975); K. L. Buchan and E. J. Schwarz, *Geol. Soc. Can. Spec. Pap.* **34**, 221 (1987).
7. D. J. Dunlop, *J. Geophys. Res.* **91**, 9569 (1986). We heated the starting material in a mixture of 80% CO_2 and 20% CO for 74 hours at 395°C to reduce the oxidized surface layer and stored it in a dessicator until the beginning of each experiment. From transmission electron micrographs, the mean particle diameter was 370 Å, with a range of 100 to 650 Å. The x-ray cell edge of (8.393 ± 0.008) Å, the Curie temperature of 575°C, and the saturation magnetization M_S of 92.2 A m^2 kg^{-1} are those of stoichiometric magnetite (*8*). The ratio (M_{RS}/M_S) of saturation remanence to saturation magnetization was 0.193 and the ratio (H_{CR}/H_C) of remanent to ordinary coercive force was 2.14. Most of the magnetite was in the SD size range; SP grains less than 250 Å in size lower the remanence ratio below and raise the coercivity ratio above the theoretical SD values of 0.5 and 1.1 to 2.0 (*9*).
8. J. Smit and H. P. J. Wijn, *Ferrites* (Wiley, New York, 1959), p. 157.
9. P. Gaunt, *Philos. Mag.* **5**, 1127 (1960).
10. Our non-inductive resistance furnace was enclosed by Helmholtz coils and located inside a mu-metal shielded room. The field could be nulled to within a few nanoteslas for long periods of time.
11. G. Bate, in *Ferromagnetic Materials*, E. P. Wohlfarth, Ed. (North-Holland, Amsterdam, 1980), vol. 2, p. 430.
12. J. M. Daniels and A. Rosencwaig, *J. Phys. Chem. Solids* **30**, 1561 (1969); H. Kojima and K. Haneda, *IEEE Trans. Magn.* **MAG-16**, 11 (1980); Y. Yamazaki *et al.*, *Adv. Ceram.* **15**, 241 (1984); K. Brown and W. O'Reilly, *J. Geophys.* **61**, 82 (1987).
13. J. E. Knowles, *J. Magn. Magn. Mat.* **22**, 263 (1981).
14. A. Michel, G. Chaudron, J. Bénard, *J. Phys.* **12**, 51 (1951).
15. A. Aharoni, E. H. Frei, M. Schieber, *J. Phys. Chem. Solids* **23**, 545 (1962).
16. Ö. Özdemir and S. K. Banerjee, *Geophys. Res. Lett.* **11**, 161 (1984).

17. R. J. Veitch, *Phys. Earth Planet. Inter.* **23**, 215 (1980); R. J. Veitch and A. Stephenson, *ibid.* **16**, 209 (1978).
18. D. J. Dunlop, *ibid.* **26**, 1 (1981), p. 5; D. J. Dunlop, *J. Geophys. Res.* **81**, 3511 (1976).
19. H. P. Johnson and R. T. Merrill, *J. Geophys. Res.* **79**, 5533 (1974); F. Heider and D. J. Dunlop, *Phys. Earth Planet. Inter.* **46**, 24 (1987).
20. W. P. Osmond, *Proc. Phys. Soc. London* **B66**, 265 (1953); D. H. Lindsley, in *Oxide Minerals*, vol. 3 of *Reviews of Mineralogy*, D. Rumble III, Ed. (Mineralogical Society of America, Washington, DC, 1976), p. L–23.
21. R. F. Butler, *J. Geophys. Res.* **78**, 6868 (1973); B. M. Moskowitz, *Earth Planet. Sci. Lett.* **47**, 285 (1980).
22. K. Haneda and H. Kojima, *J. Phys.* **40**, Colloq. C2, Suppl. 3, 583 (1979).
23. Y. Imaoka, Y. Hoshino, M. Sato, in *Ferrites* (University Park Press, Baltimore, 1970), p. 467.
24. D. J. Dunlop, *Geophys. J.* **74**, 667 (1983).
25. C. W. F. Everitt, *Philos. Mag.* **6**, 713 (1961); D. J. Dunlop and G. F. West, *Rev. Geophys.* **7**, 709 (1969).
26. D. J. Dunlop, *Rev. Geophys. Space Phys.* **11**, 855 (1973); D. J. Dunlop and J. M. Stirling, *Geophys. Res. Lett.* **4**, 163 (1977).
27. B. Gustard and W. J. Schuele, *J. Appl. Phys.* **37**, 1168 (1966); I. G. Hedley, *Phys. Earth Planet. Inter.* **1**, 103 (1968); H. Porath, *J. Geophys. Res.* **73**, 5959 (1968).
28. D. J. Dunlop, *J. Geophys.* **40**, 439 (1974); H. H. Thomas, *J. Geophys. Res.* **92**, 11609 (1987); J. Arkani-Hamed, *Geophys. Res. Lett.* **15**, 48 (1988).
29. K. L. Buchan, G. W. Berger, M. O. McWilliams, D. York, D. J. Dunlop, *J. Geomagn. Geoelectr.* **29**, 401 (1977); E. Irving and D. F. Strong, *J. Geophys. Res.* **90**, 1949 (1985); D. V. Kent and N. D. Opdyke, *ibid.*, p. 5371.
30. We thank A. McLean and M. Ward of the Department of Metallurgy and Materials Science for reducing our starting magnetites, M. Back of the Royal Ontario Museum for the x-ray analyses, and B. Head for encapsulating the VRM samples under vacuum. The project was supported by Energy, Mines, and Resources Canada research agreements and by Natural Sciences and Engineering Research Council of Canada operating grant A7709.

12 October 1988; accepted 22 December 1988

Epitaxial Growth of Diamond Films on Si(111) at Room Temperature by Mass-Selected Low-Energy C^+ Beams

J. L. ROBERTSON, S. C. MOSS, Y. LIFSHITZ,* S. R. KASI,
J. W. RABALAIS, G. D. LEMPERT, E. RAPOPORT

Diamond films (~0.7 micrometer thick) have been epitaxially grown on Si(111) substrates at room temperature with mass-selected 120-electronvolt C^+ ions. The diamond reflections observed in x-ray diffraction are well localized at their predicted positions, indicating that (i) the diamond(111) and (220) planes are parallel to the Si(111) and (220), respectively; (ii) the diamond rotational spread around its ⟨111⟩ normal is ~1.7°; and (iii) the mosaic block size is ~150 Å. The film growth is discussed in terms of subplantation—a shallow subsurface implantation model. This discovery is an important step toward diamond semiconductor devices.

AMONG THE UNIQUE PHYSICAL properties of diamond that suggest great technological promise are its wide band gap (negligible electrical conductivity) together with its high thermal conductivity (*1–4*). Diamond synthesis, which remains a challenge, has been achieved in the past 30 years by two main approaches: high pressure–high temperature synthesis (*1*) of bulk material and low pressure–medium temperature (~600° to 1000°C) synthesis (*5–6*) of thin films by chemical vapor deposition (CVD). Semiconducting diamond, an attractive material for integrated circuits, has been grown homoepitaxially on diamond substrates (*2–4*) and polycrystalline diamond films have been grown on many substrates. This has been established by several methods, including x-ray diffraction that exhibits polycrystalline cubic diamond pattern (*6*). Recent reviews of this field are now available (*2, 6–8*). Heteroepitaxial growth of diamond films on non-diamond substrates, a necessity for most electronic device applications, has not yet been reported. We provide here experimental x-ray data that demonstrates heteroepitaxial growth of a diamond film, by means of mass-selected carbon ion beam deposition, on the (111) surface of silicon at room temperature. Diamondlike films have been deposited from carbon ion beams on substrates by different groups (*9–11*). X-ray diffraction and transmission electron microscopy indicated polycrystalline (diamond) constituents with a grain size of ~100 Å coupled with some larger crystals. Preferred (111) orientation was also noted.

Recently some of us reported (*12–14*) on thin (~100 to 500 Å) diamond films grown by impinging low-energy (60 to 180 eV) mass-selected C^+ ions on room-temperature substrates in an ultrahigh vacuum. In situ surface analysis of the film growth by several techniques at the University of Houston showed the evolution of diamond sp^3 short-range order through carbidic and graphitic stages. At higher (200 to 300 eV) or lower (~10 to 30 eV) energies, much higher fluences were needed for the formation of the graphitic phase while the pure diamond sp^3 phase was not detected for practical fluences. Following this, thicker films (~1 μm) were deposited on Si(111) crystals at Soreq Nuclear Research Center with the optimal procedure determined in Houston, that is, 120-eV C^+ ions and a room-temperature substrate. The Si wafers were cleaned prior to the deposition with diluted HF to remove the oxide layer. The current density was ~400 $\mu A/cm^2$ and several hours were required for deposition. The films had a varying thickness profile, corresponding to the beam profile, and thus exhibited color fringes indicating transparency in the visible range (see Fig. 1) which argues persuasively against their being graphitic.

X-ray experiments were confined to the thicker portion of the ~0.7-μm film on Si(111) shown in the photo in order to determine the crystal phase, mosaic character, orientation, and epitaxy. Because the scattering from a 0.7-μm carbon film may be weak, it is difficult to find the carbon peaks in a casual survey alignment scan. The approach adopted here was to align on

Fig. 1. Diamond(111) film epitaxially grown on room temperature Si(111) from 120-eV mass-selected C^+ ion beam. The color interference fringes are the result of the varying thickness profile of the film. The maximum thickness is on the side where the fringes converge; the number of fringes indicate a thickness of ~7000 Å in that region.

J. L. Robertson, S. C. Moss, Department of Physics, University of Houston, Houston, Texas 77204-5504.
Y. Lifshitz, S. R. Kasi, J. W. Rabalais, Department of Chemistry, University of Houston, Houston, Texas 77204-5641.
G. D. Lempert and E. Rapoport, Soreq Nuclear Research Center, Yavne 70600, Israel.

---

*On sabbatical leave from Soreq Nuclear Research Center, Yavne 70600, Israel.